

Research Paper

Long-term effects of myo-inositol on traumatic brain injury: Epigenomic and transcriptomic studies



Nino Oganezovi^{a,1}, Vincenzo Lagani^{a,b,2}, Marine Kikvidze^{a,3}, Georgi Gamkrelidze^{a,4}, Lia Tsverava^{a,5}, Eka Lepsveridze^{a,6}, Kevin M. Kelly^{c,d,e,f,7}, Revaz Solomonias^{a,g,*,8}

^a School of Natural Sciences and Medicine, Institute of Chemical Biology, Ilia State University, Tbilisi, Georgia

^b Biological and Environmental Sciences and Engineering Division, King Abdullah University of Science and Technology, Thuwal 23955, Saudi Arabia

^c Department of Neurobiology and Anatomy, Drexel University College of Medicine, Philadelphia, PA, United States

^d Department of Neurology, Philadelphia, PA, United States

^e Department of Neurology, Allegheny General Hospital, Pittsburgh, PA, United States

^f Center for Neuroscience Research, Allegheny Health Network Research Institute, Pittsburgh, PA, United States, Drexel University College of Medicine, Philadelphia, PA, United States

^g Iv. Beritashvili Centre of Experimental Biomedicine, Tbilisi, Georgia

ARTICLE INFO

Keywords:

Traumatic Brain Injury
DNA methylation
Gene expression
Myo-inositol
BATF2

ABSTRACT

Background and purpose: Traumatic brain injury (TBI) and its consequences remain great challenges for neurology. Consequences of TBI are associated with various alterations in the brain but little is known about long-term changes of epigenetic DNA methylation patterns. Moreover, nothing is known about potential treatments that can alter these epigenetic changes in beneficial ways. Therefore, we have examined myo-inositol (MI), which has positive effects on several pathological conditions.

Methods: TBI was induced in mice by controlled cortical impact (CCI). One group of CCI animals received saline injections for two months (TBI+SAL), another CCI group received MI treatment (TBI+MI) for the same period and one group served as a sham-operated control. Mice were sacrificed 4 months after CCI and changes in DNA methylome and transcriptomes were examined.

Results: For the first time we: (i) provide comprehensive map of long-term DNA methylation changes after CCI in the hippocampus; (ii) identify differences by methylation sites between the groups; (iii) characterize transcriptome changes; (iv) provide association between DNA methylation sites and gene expression. MI treatment is linked with upregulation of genes covering 33 biological processes, involved in immune response and inflammation. In support of these findings, we have shown that expression of BATF2, a transcription factor involved in immune-regulatory networks, is upregulated in the hippocampus of the TBI+MI group where the BATF2 gene is demethylated.

Conclusion: TBI is followed by long-term epigenetic and transcriptomic changes in hippocampus. MI treatment has a significant effect on these processes by modulation of immune response and biological pathways of inflammation.

Abbreviations: TBI, Traumatic Brain Injury; CCI, controlled cortical impact; MI, Myo-inositol; DNMT, DNA methyltransferases; RRBS, Reduced-representation bisulfite sequencing; SDS, sodium dodecyl sulphate.

* Corresponding author at: School of Natural Sciences and Medicine, Institute of Chemical Biology, Ilia State University, Tbilisi, Georgia.

E-mail address: revaz_solomonias@iliauni.edu.ge (R. Solomonias).

¹ 0009-0006-5764-6795

² 0000-0002-6552-6076

³ 0009-0005-8594-3861

⁴ 0000-0002-0965-0363

⁵ 0000-0001-5545-8009

⁶ 0000-0001-8991-4666

⁷ 0000-0001-7505-0561

⁸ 0000-0003-4798-6762

<https://doi.org/10.1016/j.ibneur.2024.01.009>

Received 10 November 2023; Accepted 27 January 2024

Available online 30 January 2024

2667-2421/© 2024 The Author(s). Published by Elsevier Inc. on behalf of International Brain Research Organization. This is an open access article under the CC BY-NC-ND license (<http://creativecommons.org/licenses/by-nc-nd/4.0/>).

1. Introduction

Traumatic brain injury (TBI) is a serious health issue that can affect people of any age all over the world. TBI can frequently result in long-term disabilities or death and involve a spectrum of brain abnormalities from acute to chronic. Consequences of TBI can be diverse and include post-traumatic epilepsy (PTE) (After and Brain, 1998), neurodegenerative diseases (Kenborg et al., 2015), psychiatric problems (McLean et al., 1984), neuroendocrine impairment (Vespa, 2013), and sleep disorders (Masel et al., 2001). All these consequences are linked to the long-term electrophysiological, morphological, biochemical, and molecular biological alterations (Rakib et al., 2021; Ratliff et al., 2020; Ustaoglu et al., 2021). Among processes associated with TBI that can intensively influence long-lasting cellular activity are epigenetic alterations, which play a key role in regulation of gene expression at many different levels, including transcription and post-transcriptional modifications, as well as translation and post-translational modifications (Monsour et al., 2022; Zima et al., 2022). The main mechanisms of epigenetic modifications include DNA methylation and demethylation, post-translational histone modification, and the actions of non-coding RNAs such as microRNAs (Monsour et al., 2022). DNA methylation is a process involving the covalent transfer of a methyl group to the C-5 position of the cytosine ring of DNA. The process is mediated by DNA methyltransferases (DNMTs) and is one of the key mechanisms of epigenetic regulation (Jin et al., 2011). DNA methylation mainly suppresses expression of the corresponding gene, but it is very much context dependent. The locus of methylation as well as the type of stimulus can influence the transcriptome of the cell differently (Dhar et al., 2021). Epigenetic changes are vastly studied in diverse pathological conditions since they can be reversed by pharmacological interventions, which makes them interesting targets for possible treatments. Study of epigenetic modifications after TBI has recently drawn much attention, but this investigation is still in its infancy (Zima et al., 2022), especially since little is known about long-term effects of TBI on DNA methylation. It is obvious that finding treatments that counteract epigenetic changes that lead to the pathological outcomes of TBI is of great importance. As far as we know, no such treatment is currently available.

Myo-inositol (MI) is one of nine isomers of the cyclohexane family. It is present in the human body, including the nervous system (Bizzarri et al., 2016). MI and its derivatives participate in diverse physiological processes, such as endocrine modulation, developmental processes, and calcium metabolism. Various conditions have been reported to benefit from MI treatment, such as depressive disorders (Taylor et al., 2004), and polycystic ovary syndrome (Unfer et al., 2017). Moreover, anti-epileptogenic properties of MI have been shown in our previous studies performed on pharmacological (kainic acid-KA) animal models of epilepsy (Kandashvili et al., 2022; Tsverava et al., 2019, 2016). It should be emphasized that MI has a long-term influence on KA-induced alterations since its beneficial effects are maintained for at least 1 month after its treatments end (Kandashvili et al., 2022; Tsverava et al., 2019).

In line with these data, we have hypothesized that MI could also exert its long-term effects on TBI-induced epigenetic and transcriptomic changes.

There are several models of TBI and controlled cortical impact (CCI) is among them. CCI enables a strong control over impact parameters and guarantees the application of similar injury to all experimental objects (Hunt et al., 2009; Kelly et al., 2015). The CCI model has been used to study different aspects of TBI and its consequences at different levels from behavioral to cellular.

The present study's objectives were to determine whether: (i) CCI is followed by long-term changes in DNA methylation and characterize these sites and; (ii) MI treatment after CCI exerts long-term effects on DNA methylation and gene expression patterns. We have also investigated whether there is an inverse correlation between DNA methylation and gene expression patterns on a selected protein level.

Experiments were performed on adult (2–3 month-old) mice using

CCI and followed by MI treatment for two months, the most susceptible period during which the main pathological changes take place and lead to severe consequences, including posttraumatic spontaneous seizures (Smith, 2016). To investigate long-term outcomes of TBI and the effects of MI treatment, animals were sacrificed four months after CCI. This time point allowed us to identify: (i) what type of epigenetic and gene expression alterations remain as a long-term consequences of TBI and (ii) whether 2-month MI treatment shows long-lasting effects, similar to the KA model, months following treatment termination. Biochemical and molecular biological analysis were performed on cortical and hippocampal samples taken from both hemispheres. The reason for choosing these structures was that the cortex is severely injured by the CCI procedure, which subsequently is associated with pathological changes in the hippocampus (Kharlamov et al., 2011; Mtchedlishvili et al., 2010; Osier and Dixon, 2016).

Our results convincingly demonstrate that after CCI: (i) long-term epigenetic and transcriptomic changes take place in the hippocampus of traumatized mice; (ii) MI treatment has long-lasting effects on these epigenetic and transcription alterations; (iii) for a number of genes the changes in DNA methylation and gene expression are inversely correlated.

2. Materials and methods

2.1. Traumatic Brain Injury

CCI was applied by pneumatic impact device model AMS 201 with an automatic average rod speed measurement unit (AmScien Instruments). For induction of severe TBI, compression of the cortex was applied to a depth of 1.0 mm at a velocity of 3.5 m/sec and duration of 400 ms. Picture of the damaged brain four months after application of CCI is provided in [Supplementary Fig. S1](#). Such a precise control over impact parameters provides standardization of the procedure, thus providing identical impact on all experimental animals. Sham-operated mice underwent identical anesthetic and surgical procedures without CCI.

After impact, animals were housed individually with a 24-hour light/dark cycle and half of them received intraperitoneal injections of 30 mg/kg MI two times daily for the following two months. This covered the most susceptible time for development of pathological changes leading to severe consequences (see Introduction). To determine whether: (i) CCI has a long-lasting effects on epigenetic changes and (ii) MI effects remain after the termination of treatment, experimental animals were sacrificed four months after CCI, which for the MI-treated animals corresponds to 2 months after ceasing intraperitoneal injections. Hippocampal and neocortical samples were extirpated for molecular-biological and biochemical analysis. DNA methylation and RNA-SEQ studies were done on mixed hippocampal samples taken from both hemispheres of each animal, whereas Western Blot analysis was done on each hemisphere sample separately. The general scheme of experiments is provided on [Fig. 1](#).

2.2. Reduced-representation bisulfite sequencing (RRBS)

The RRBS experiment was conducted on 9 hippocampal samples (3 samples from each of TBI+SAL, TBI+MI and CON+SAL groups). DNA Methylation Profiling (RRBS Service) (Diagenode Cat# G02020000) was applied for this purpose.

2.2.1. Genomic DNA quality control

DNA concentration of the samples was measured using the Qubit® dsDNA HS Assay Kit (Thermo Fisher Scientific) and DNA quality of the samples was assessed with the Fragment Analyzer™ and the DNF-488 High Sensitivity genomic DNA Analysis Kit (Agilent).

2.2.2. RNase treatment

Genomic DNA from 9 selected samples was treated with RNase

cocktail (Thermo Fisher Scientific, AMM2288) for 30 min at 37 °C to remove contaminating small RNAs. Following the treatment, DNA was purified using Agencourt AmpureXP beads (Beckman Coulter). DNA was eluted in Elution Buffer (10 mM Tris-Cl, pH 8.5) and quality control steps were performed as described above.

2.2.3. RRBS library preparation

The RRBS library preparation was performed by DNA Methylation Profiling Service (RRBS Service) (Diagenode Cat# G02020000). The Premium Reduced Representation Bisulfite Sequencing (RRBS) v2 Kit (Diagenode Cat# C02030036) was used for RRBS libraries preparation. 100 ng of genomic DNA were used to start library preparation for each sample. PCR clean-up after the final library amplification was performed using a 1.45x beads:sample ratio of Agencourt® AMPure® XP (Beckman Coulter).

2.2.4. RRBS library pools quality control

DNA concentration of the pools was measured using the Qubit® dsDNA HS Assay Kit (Thermo Fisher Scientific). The profile of the pools was checked using the DNF-474 NGS fragment kit on a Fragment Analyzer (Agilent).

In the event of adapter dimer peaks being too high, the pools were size-selected one more time using a 1.45x beads:sample ratio of Agencourt® AMPure® XP (Beckman Coulter) and quality control steps were performed again.

2.2.5. Deep sequencing

RRBS library pools were sequenced on a NovaSeq6000 (Illumina) using 50 bp paired-end read sequencing (PE50).

2.3. RNA-SEQ

The RNA-SEQ experiment on 6 hippocampal samples (3 samples from TBI+SAL and 3 samples from TBI+MI groups) was performed by RNA-SEQ services (Diagenode Cat# G02030000). RNAs were extracted using the RNeasy Mini kit (Qiagen #74104). RNA was quantified using Qubit™ RNA BR Assay Kit (Thermo Fisher Scientific, Q10210) and secondarily checked for integrity using RNA 6000 Pico Kit (5067–1513, Agilent) on a 2100 Bioanalyzer system (Agilent).

The 6 samples were processed together and library preparation was done with 500 ng of input RNA using: NEBNext® rRNA Depletion Kit (Human/Mouse/Rat) (NEB #E6310) followed by NEBNext Ultra II Directional RNA Library Prep Kit for Illumina (NEB #E7760) and NEBNext® Multiplex Oligos for Illumina® Index Primers Set 1 (NEB# E6440). Optimal library amplification was assessed by qPCR on Light-Cycler® 96 System (Roche). The generated DNA libraries were purified using Agencourt® AMPure® XP (Beckman Coulter). Purified libraries were quantified using Qubit™ dsDNA HS Assay Kit (Thermo Fisher Scientific, Q32854) and their size assessed with QIAxcel (Qiagen). Illumina sequencing was applied with paired-end 50 bp 50 M raw reads/sample on average (Diagenode Cat# G02030003).

2.4. SDS electrophoresis and Western immunoblotting

SDS electrophoresis and Western immunoblotting experiments were performed on the whole homogenate fractions from the hippocampal and neocortical samples separately from each hemisphere. Three groups of experimental mice (CON+SAL, TBI+SAL and TBI+MI) were analyzed. Brain tissues were rapidly homogenized in 0.32 M sucrose, 20 mM Tris-HCl (pH 7.4), cocktail of protease inhibitors (Sigma, P8340), 1 mM ethylenediaminetetraacetic acid, 1 mM sodium orthovanadate, 10 mM sodium pyrophosphate and 0.5 mM ethylene glycol-bis(2-aminoethylether)-N,N,N',N'-tetraacetic acid. The protein concentration was determined in brain tissue homogenate fractions in quadruplicate, using a micro bicinchoninic acid protein assay kit (Pierce).

Samples containing 30 µg protein in equal volumes were applied to the sodium dodecyl sulphate (SDS) gels and electrophoresis and Western blotting were performed as described previously (Solomon et al., 2013). Proteins were transferred onto nitrocellulose membranes, stained with Ponceau S solution, and analyzed with Image J software (<https://imagej.net/ImageJ>) to confirm uniform gel loading and transfer. Standard immunochemical procedures were performed using primary antibodies against BATF2 (PA5–37138 (Invitrogen)) and peroxidase-labelled secondary antibodies and Super-Signal West Pico Chemiluminescent substrate (Pierce) (Solomon et al., 2013, 2010). The optical densities of bands corresponding to BATF2 were measured using LabWorks 4.0 (Ultra-Violet Products Ltd., Cambridge, UK). The autoradiographs were calibrated by including in each gel four standards of homogenate (15, 30, 45, and 60 µg of corresponding total protein) obtained from the control mice. Optical density was proportional to the amounts of BATF2 (see Fig. 5). For the data analysis optical density of each sample band was divided by the optical density of the band for 30 µg of protein standard (Solomon et al., 2013, 2010) to give “relative amount of protein.”

We have not normalized obtained density data with respect to any other housekeeping protein in brain tissue samples because it cannot be guaranteed that such proteins are not affected by CCI e.g. (Li and Shen, 2013). As outlined above, the gel loading was controlled by Ponceau S staining, Image J software analysis, and calibration with protein standards.

2.5. Bioinformatics analysis

Raw fastq files were processed with nf-core pipelines (Di Tommaso et al., 2017; Ewels et al., 2020)]. The nf-core “methyleseq” pipeline was used for the RBBS-seq data; this pipeline uses “Trim Galore!” for trimming adapter sequences, and Bismark (Krueger and Andrews, 2011) for reads alignment and methylation calls. In contrast, the nf-core “rnaseq” pipeline used for the transcriptomics profiling is based upon “Trim Galore!,” the combination of STAR (Dobin et al., 2013) and Salmon (Patro et al., 2017) for reads alignment and expression levels quantification. The ENSEMBL mm10 version 81 reference mouse genome was used for alignment.

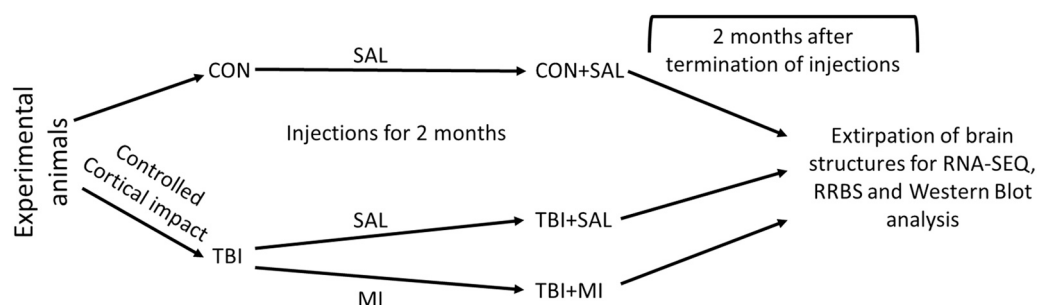


Fig. 1. The general scheme of experiments.

2.6. Statistical analysis

The R package BiSeq (Hebestreit et al., 2013) was used for extracting methylation levels from the coverage files produced by the Bismark aligner, and for smoothing methylation levels within CpG clusters. The moderated t-statistics implemented in the limma package (Ritchie et al., 2015) was employed for identifying differentially methylated CpG sites between each pair of experimental conditions. Log-transformed methylation values (a.k.a. “m-values”) were for differential analysis, as their distributional properties better adhere to t-test assumptions (Du et al., 2010). CpG sites were associated with the closest gene, considering a window of 2000 base-pairs upstream of each gene TSS as the promoter region.

Normalization and differential expression analysis of RNA-seq counts data were performed with the R package DESeq2 (Love et al., 2014). The hypergeometric test (Wu et al., 2021) was used for identifying Gene Ontology (Ashburner et al., 2000) biological process enriched for differentially expressed/methylated gene. A 0.1 False Discovery Rate threshold was consistently used for assessing statistical significance.

All statistical analyses were performed using the R Statistical Software (R Development Core Team, 2016).

The protein data were analyzed by one-way ANOVA with factor-treatment (TBI+SAL; TBI+MI and CON+SAL). In the event of a significant effect in ANOVA, planned comparisons were done by two-tailed t-test.

3. Results

3.1. TBI+SAL and TBI+MI treatments are associated with profound but different changes in DNA methylation

The RRBS-SEQ experiments provided methylation levels over 1185807 CpG sites. The methylation profiles of the control samples were highly similar, whereas the TBI+SAL and TBI+MI groups showed more heterogeneity (Supplementary Fig. S2).

The comparison between each pair of experimental conditions highlighted the presence of several TBI-associated changes in the methylome: 597 when contrasting TBI+MI vs. TBI+SAL, 851 in TBI+SAL vs. Controls, and 980 for TBI+MI vs. Controls (FDR adjusted p-value ≤ 0.1 ; Fig. 2a; Supplementary Tables S1, S2, and S3, respectively).

Fig. 2b indicates that some changes are unique with respect to each group. In particular, 542 CpG sites are hypermethylated in both TBI+SAL and TBI+MI compared with control samples, 156 CpG sites are hypomethylated exclusively in TBI+SAL hippocampus, and 314 CpG sites are hypomethylated exclusively in the TBI+MI group (lists of uniquely deregulated CpG sites are in Supplementary Table S4).

The unique methylation changes cover different molecular pathways (see Fig. 3, Supplementary Fig. S3, and Supplementary Table S5, S6, and S7). Interestingly, 7 Gene Ontology (GO) Biological Processes are enriched for hypermethylated CpG sites both in the TBI+SAL vs. CON+SAL contrast, and in the TBI+MI vs. CON+SAL contrast, including: dynein intermediate chain binding, dynein light intermediate chain binding, histone deacetylase binding, microtubule motor activity, minus-end-directed microtubule motor activity, ubiquitin conjugating enzyme activity, and ubiquitin-like protein conjugating enzyme activity. Conversely, when TBI+MI and TBI+SAL are contrasted against each other, 46 GO biological processes are enriched for hypermethylated CpG sites, most notably C-acyltransferase activity, SH3 domain binding, ADP binding, NAD binding, exopeptidase activity, and oxidoreductase activity acting on the CH-OH group of donors, and NAD or NADP as acceptor. The comparison of hypomethylated CpG sites between the same groups reveals 25 biological processes enriched in the TBI+MI group. These biological processes include core promoter sequence-specific DNA binding, transcription corepressor activity, transmembrane transporter binding, ion channel inhibitor activity, tau

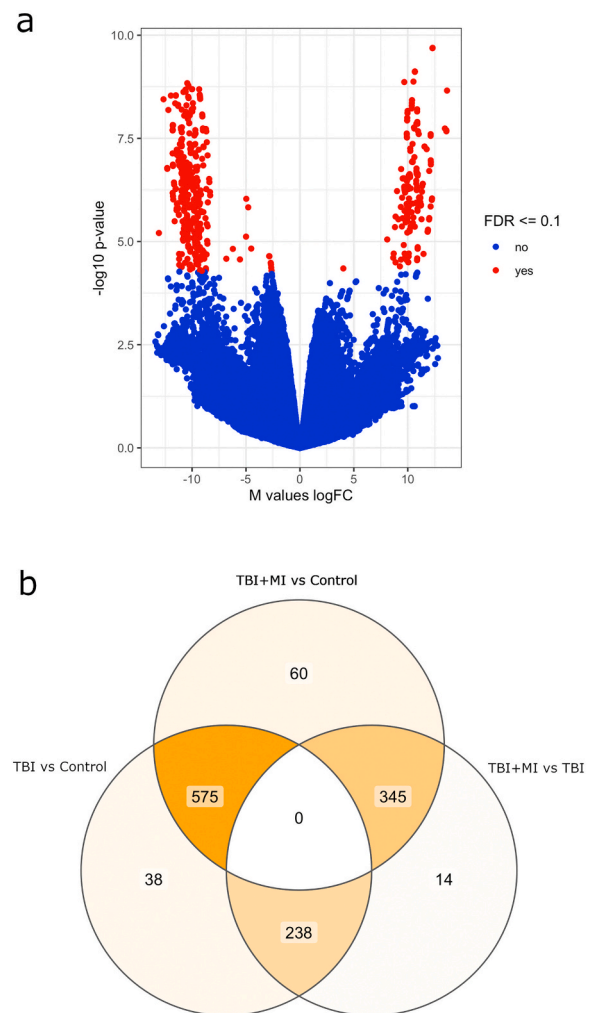


Fig. 2. : Methylation changes. a) Volcano plot of methylation differences between TBI+MI and TBI+SAL. Each dot represents a CpG site, x-axis log fold change in M-values, y-axis statistical significance. Positive log FC indicates hypermethylation in TBI+MI; gray dots are significant CpG (FDR adjusted p-value ≤ 0.1), black not significant. b) Venn diagram showing overlapping among deregulated CpGs across the three contrasts. Both hyper- and hypomethylated CpG are considered (FDR adjusted p-value ≤ 0.1).

protein binding, and many others.

Finally, we identified GO biological processes that are enriched on CpG sites showing methylation changes specific for each group. Biological processes enriched for CpG sites hypermethylated in both TBI+SAL vs. CON+SAL and TBI+MI vs. CON+SAL are listed in Supplementary Table S8. Analysis of CpG sites hypomethylated exclusively in TBI+SAL (Supplementary Table S9) results in a total of 44 enriched biological processes, most notably exopeptidase activity and SH3 domain binding. Considering CpG sites hypomethylated exclusively in TBI+MI (Supplementary Table S10) instead results in a total of 79 enriched biological processes, including core promoter sequence-specific DNA binding, histone deacetylase binding, helicase activity, and many others.

3.2. TBI+SAL and the TBI+MI groups have different transcriptomic profiles

PCA analysis identified a TBI+MI sample whose expression profile appeared to be identical to TBI+SAL samples, and therefore was discarded as an outlier (Supplementary Fig. S4).

A total of 378 genes were differentially expressed (FDR adjusted p-

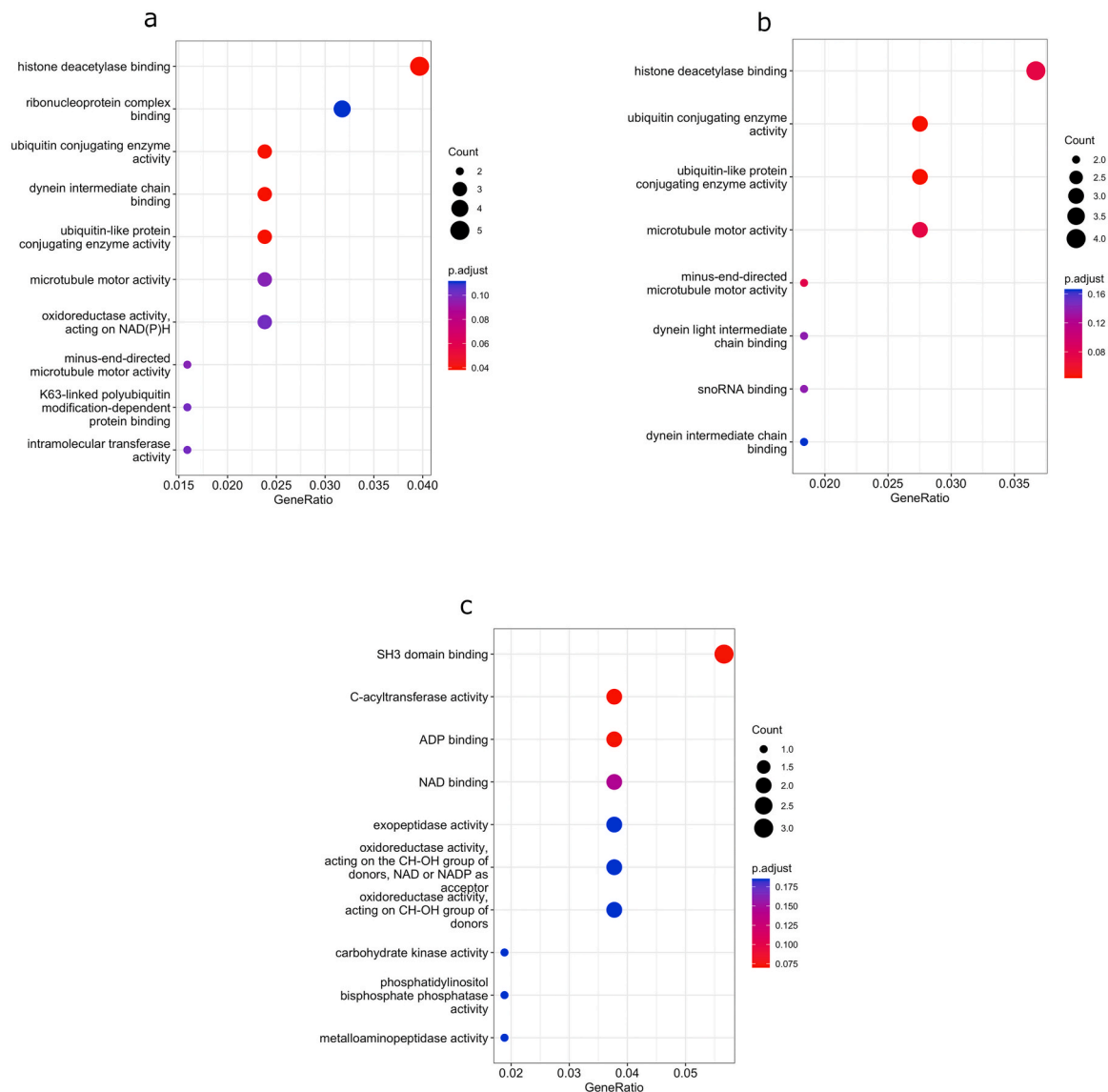


Fig. 3. : Gene Ontology biological processes enrichment for hypermethylated CpG sites. Each dot represents a biological process. The x-axis reports the ratio of genes linked to hypermethylated CpG sites that are also in the biological process. The size of the dots reports the absolute number of hypermethylated genes. Panel a) corresponds to the TBI+SAL vs. CON+SAL contrast, panel b) to the TBI+MI vs. CON+SAL contrast, and panel c) to the TBI+MI vs. TBI+SAL contrast.

value ≤ 0.1) between the TBI+MI and TBI+SAL groups (Fig. 4a and Supplementary Table S11). Of these 378 genes, 347 are overexpressed in TBI+MI, with a total of 33 GO biological processes enriched for these 347 genes (see Figs. 4b, 4c and Supplementary Table S12), whereas downregulated genes covered 23 biological processes (Supplementary Table S13).

3.3. Some differentially expressed genes are overlapping with demethylated CpG sites in hippocampus after TBI+SAL and TBI+MI treatment

Overlap between demethylated CpG sites and differentially expressed genes is limited. We identified 49 genes for which expression was significantly deregulated (FDR adjusted p-value 0.1) with CpG sites showing demethylation that is nominally significant (unadjusted p-value 0.05, Supplementary Table 14). Among these, 24 genes display an inverse relationship between expression and methylation. In particular, the BATF2 gene is overexpressed in TBI+MI with respect to TBI+SAL, whereas all CpG sites constituting a CpG island located between its first two exons are hypomethylated. BATF2 differential expression was

further validated through Western Blot analysis.

3.4. BATF2 levels are increased in the ipsilateral hippocampus of TBI+MI group

Anti-BATF2 antibodies bound to a protein band with a molecular weight of 29 kDa, which corresponds to the expected size of target protein. For the applied four internal standards, the least-squares regression showed a significant fit to a straight line (Fig. 5).

In the ipsilateral hippocampus the effect of treatment on the amount of BATF2 was significant (one-way ANOVA $F_{2,17} = 3.88$, $P = 0.044$). The planned comparisons revealed that level of the studied protein was significantly higher in the hippocampus of the TBI+MI group compared with the TBI+SAL group ($T = 2.46$, $P = 0.034$, $DF = 10$, Fig. 5). The difference between the TBI+MI and CON+SAL groups was similar, but significant only with a one-tailed test, whereas nearly the same levels of the BATF2 were observed in the TBI+SAL and CON+SAL groups (see Supplementary Table S15).

No significant effect of treatment in one-way ANOVA was observed for other three brain regions (see Supplementary Table S15).

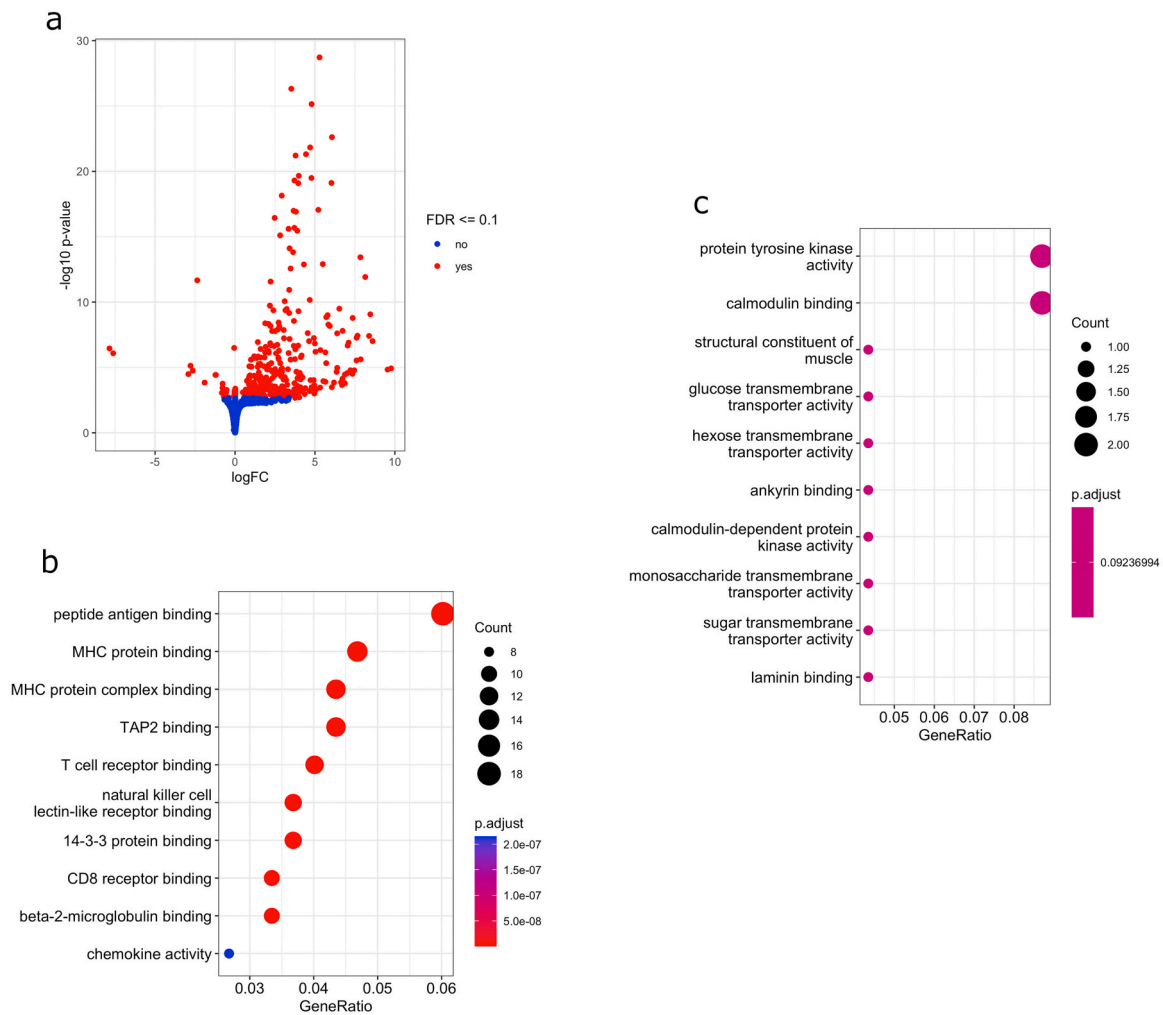


Fig. 4. : Expression changes. a) Volcano plot of expression differences between TBI+MI and TBI. Each dot represents a gene site, x-axis log fold change, y-axis statistical significance. Positive log FC indicates overexpression in TBI+MI; red dots are significant genes (FDR adjusted p-value ≤ 0.1), blue not significant. b) Gene Ontology biological processes enriched for significantly upregulated genes. Each dot represents a biological process. The x-axis reports the ratio of differentially expressed genes that are also in the biological process. The size of the dots reports the absolute number of differentially expressed genes. c) Gene Ontology biological processes enriched for significantly downregulated genes. Details as in b).

4. Discussion

Traumatic brain injury is known for its long-term consequences that can be associated with various problems, including inflammatory events, post-traumatic seizures, demyelination, and apoptosis (Bramlett and Dietrich, 2015). The hippocampus is one of the most susceptible brain structures that demonstrates a variety of alterations after TBI. This has been shown by results obtained from experimental models of TBI as well as from humans (Atkins, 2011; Kharlamov et al., 2011; Mtchedlishvili et al., 2010). The damages occurring in the hippocampus after brain injury can be unilateral or bilateral and can have diverse representations (Ariza et al., 2006; Ngwenya and Danzer, 2019).

Our data for the first time: (i) convincingly indicate long-term epigenetic alterations in the hippocampus of TBI in mice; (ii) provide a detailed map of altered methylation sites; (iii) characterize transcriptome changes; (iv) provide association between DNA methylation sites and gene expression and (v) reveal MI effects on these changes. We have quantified methylation across more than 1 million CpG sites 4 months after TBI and nearly a thousand methylation sites are significantly altered by TBI. By methylation signature, TBI+SAL and TBI+MI groups are clearly different from the control group. The majority of these differences are shared by TBI+SAL and TBI+MI groups, which reflect the effects of TBI itself. The TBI+SAL and TBI+MI groups differ from

each other to a less extent, with a total of nearly 600 sites with significantly different methylation levels which indicates a long-term epigenetic effects of MI treatment on TBI. These differences include both hyper- and hypomethylated sites.

Abnormal hypermethylation at specific DNA sequences can serve as biomarkers for.

a variety of diseases (reviewed in (Ehrlich, 2019)). Disease-associated DNA hypermethylation can modulate gene expression in both directions - down-regulate or up-regulate it (Ehrlich, 2019). Therefore we cannot conclude that all DNA hypermethylated sites are ultimately associated with gene expression repression.

Altered methylation sites identified in our experiments cover genes and nearby regions from a number of biological processes (see Supplementary Tables S4-S10). TBI+SAL and TBI+MI are different from the CON+SAL group by biological processes involving dynein protein binding, histone deacetylase binding partners, microtubule protein activity, and proteasome components.

DNA methylation can proceed side-by-side preceding or following chromatin epigenetic changes, which especially include histone modifications and transcription regulation (Ehrlich, 2019). The identified differences by histone deacetylase binding partners demonstrate that profound long-term epigenetic changes occur after TBI.

Available data indicate that protein products of genes and pathways

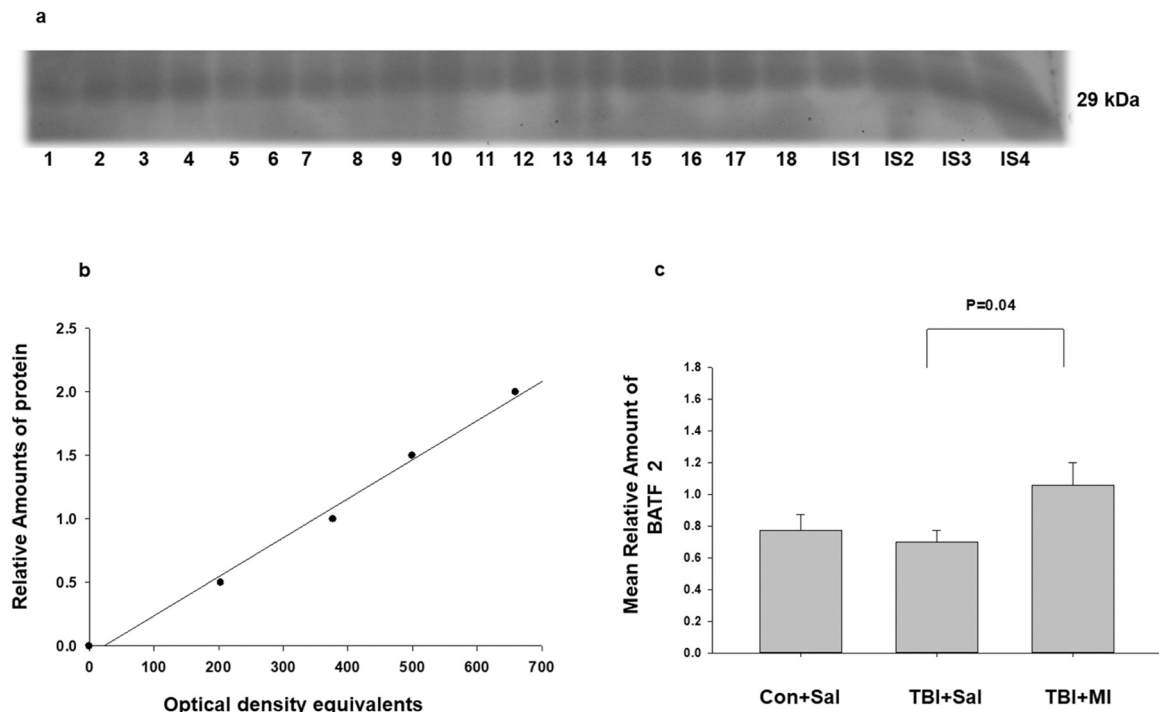


Fig. 5. : BATF2 protein expression levels in the ipsilateral hippocampus of CON+SAL, TBI+SAL, and TBI+MI groups. a) Sample film: each lane contains an individual sample. Lanes IS1-IS4 show internal standards containing 15, 30, 45 and 60 μ g of protein, respectively. b) The calibration plot was fitted by a linear least-squares regression. c) Statistical comparison of the mean levels of BATF2 (mean \pm standard error of the mean).

listed above are changed after TBI. For example, forensic autopsies from TBI victims have shown strong decreases of dynein, dynactin, and kinesin proteins (Olczak et al., 2019). The authors suggest that immunostaining for dynein, dynactin, and kinesin should be considered as a supplemental diagnostic tool for TBI in postmortem neuropathological examinations (Olczak et al., 2019).

The alteration of microtubule dynamics in neurodegenerative diseases, including TBI, is well documented (Brunden et al., 2017). Our data indicate that these alterations could be of a long-term nature and maintained by epigenetic mechanisms.

Proteasome activity and component changes were studied within 1 week after TBI (Yao et al., 2008). Proteasome activity assays revealed that peptidyl glutamyl peptide hydrolase-like and chymotrypsin-like activity were significantly decreased in the CNS following TBI, but trypsin-like proteasome activity was increased in the injured cerebral cortex. Bidirectional changes were also observed for the levels of proteasome protein components. Thus TBI affects both proteasome composition and function (Yao et al., 2008). Our data suggest that proteasome changes are also of a long-term nature.

Notably, the significant differences between TBI+SAL and TBI+MI groups include methylation sites not found in the other contrasts, and hence other biological pathways as well. Differentially hypermethylated sites in the TBI+MI group compared with the TBI+SAL group encompass 46 GO biological processes, including C-acyltransferase activity, SH3 domain binding, ADP binding, NAD binding, exopeptidase activity, oxidoreductase activity, acting on the CH-OH group of donors, and NAD or NADP as acceptor. Conversely, specifically hypomethylated sites in the TBI+MI group compared with the TBI+SAL encompass different biological processes, among them are transcription repression, transmembrane transport, ion channel inhibitor activity, tau protein binding, and many others. We suggest that these differences are the effects of MI treatment specific for TBI, rather than the changes induced by MI treatment in general, e.g., on healthy controls. This assumption is supported by our data in which CON+SAL and CON+MI groups were never different from each-other by any studied biochemical changes evoked by

kainic acid treatment (Tsverava et al., 2019).

RNA-SEQ data support the assumption that after TBI MI exerts long-lasting specific effects on chromatin activity. The expression of nearly 350 genes are increased in the hippocampus of the TBI+MI group compared with the TBI+SAL group, whereas only 29 are decreased. Upregulated genes cover 29 GO biological processes, the majority among them are processes involved in immune response and inflammation (e.g., peptide antigen binding, MHC protein complex binding, T cell receptor binding, cytokine binding, chemokine activity, immune receptor activity, and many others). Downregulated genes processes (33 in total) include protein tyrosine kinase activity, calmodulin binding, hexose transmembrane transporter activity, and others.

Cytokines are a class of small proteins that act as signaling molecules at picomolar or nanomolar concentrations to regulate inflammation and modulate cellular activities such as growth, survival, and differentiation. Chemokines are a family of low molecular weight chemotactic cytokines that regulate leukocyte migration through interactions with seven-transmembrane, G protein-coupled receptors (Zlotnik and Yoshie, 2000). They are produced mainly by microglia [48]. The dysregulation of cytokines and chemokines is a central feature in the development of neuroinflammation, neurodegeneration, and demyelination both in the central and peripheral nervous systems (Ramesh et al., 2013). Cytokines and chemokines can help to mobilize the adaptive immune response and often inflammation may induce beneficial effects such as phagocytosis of apoptotic cells. It is well established that a critical balance between repair and proinflammatory factors determines the outcome of a neurodegenerative process (Ramesh et al., 2013). Based on our previous results of the neuroprotective action of MI after KA-induced SE (Kandashvili et al., 2022; Tsverava et al., 2016) we speculate that profound changes in gene expression in the MI+TBI group could be of some benefit by mitigating the destructive effects of TBI.

For 24 upregulated genes in the hippocampus of the TBI+MI group, our RRBS-seq experiments revealed demethylation conditions. For further studies we have chosen the BATF2 transcription factor. It belongs to the family of transcription factors that includes also Basic

leucine zipper transcription factor ATF-like (BATF) and BATF3. They are involved in the regulation of numerous cellular processes, including the control of immune-regulatory networks (Murphy et al., 2013). Recently it has been shown that loss of BATF2 in humans is associated with a neurological phenotype. Authors of the study consider BATF2 as a novel disease-associated gene for severe epilepsy and mental retardation related to dysregulation of immune responses (Zsurka et al., 2023). In our study, the level of BATF2 is significantly upregulated in the ipsilateral hippocampus of the TBI+MI group compared with the TBI+SAL group. These data support the results of RNA-SEQ studies and indicate the upregulation of immune-regulatory networks in the TBI+MI group.

5. Conclusion

This study shows that TBI via CCI is followed by a strong, long-lasting epigenetic and transcriptomic changes in the hippocampus of the mice. Selected biological pathways from these changes are counteracted by MI action, which could pave way for further targeted treatment of TBI pathological consequences.

Ethics approval and consent to participate

All experimental procedures were conducted in accordance with the European Communities Council Directive Guidelines for the care and use of Laboratory animals (2010/63/EU—European Commission) and approved by the animal care and use committee at the Iv. Beritashvili Center of Experimental Biomedicine.

Consent to participate

Not applicable.

Ethics approval

Experimental design was approved by the Bioethics Committee of Iv. Beritashvili Centre of Experimental Biomedicine (Protocol N 03/11.06.2020).

Consent for publication

All co-authors have agreed to the submission of the final manuscript.

Funding

Supported by the Sh. Rustaveli National Science Foundation, Georgia (SRNSFG): Grant - # [FR-19–5429]. K.M.Kelly was supported by NINDS: 1R21NS121706A1 2022–2023.

CRedit authorship contribution statement

Conceptualization - R.S., E.L., and K.K. Methodology, N.O., G.G., E.L. and V.L.; Bioinformatics analysis-V.L.; Formal analysis- V.L. E.L. and R. S.; Investigation, N.O., M.K., E.L. L.T and G.G.; Data curation, V.L. and E. L.; Writing – original draft, V.L., R.S., E.L., K.K.; Writing – review & editing, R.S., V.L., E.L. and G.G.; Visualization, M.K. N.O. E.L.; Supervision, R.S., E.L., and V.L., Funding acquisition, E.L.

Declaration of Competing Interest

None.

Data Availability

All primary data are provided in Supplementary Materials.

Appendix A. Supporting information

Supplementary data associated with this article can be found in the online version at doi:10.1016/j.ibneur.2024.01.009.

References

- After, S., Brain, T., 1998. A population-based study of seizures after traumatic. *Brain N. Engl. J. Med.* 338, 8–12.
- Ariza, M., Serra-Grabulosa, J.M., Junqué, C., Ramírez, B., Mataró, M., Poca, A., Bargalló, N., Sahuquillo, J., 2006. Hippocampal head atrophy after traumatic brain injury. *Neuropsychologia* 44, 1956–1961. <https://doi.org/10.1016/j.neuropsychologia.2005.11.007>.
- Ashburner, M., Ball, C.A., Blake, J.A., Botstein, D., Butler, H., Cherry, J.M., Davis, A.P., Dolinski, K., Dwight, S.S., Eppig, J.T., Harris, M.A., Hill, D.P., Issel-Tarver, L., Kasarskis, A., Lewis, S., Matese, J.C., Richardson, J.E., Ringwald, M., Rubin, G.M., Sherlock, G., 2000. Gene ontology: tool for the unification of biology. *Gene Ontol. Consortium Nat. Genet.* 25, 25–29. <https://doi.org/10.1038/75556>.
- Atkins, C.M., 2011. Decoding hippocampal signaling deficits after traumatic brain injury. *Transl. Stroke Res.* 2, 546–555. <https://doi.org/10.1007/s12975-011-0123-z>.
- Bizzarri, M., Fuso, A., Dinicola, S., Cucina, A., Bevilacqua, A., 2016. Pharmacodynamics and pharmacokinetics of inositol(s) in health and disease. *Expert Opin. Drug Metab. Toxicol.* 12, 1181–1196. <https://doi.org/10.1080/17425255.2016.1206887>.
- Bramlett, H.M., Dietrich, W.D., 2015. Long-term consequences of traumatic brain injury: current status of potential mechanisms of injury and neurological outcomes. *J. Neurotrauma* 32, 1834–1848. <https://doi.org/10.1089/neu.2014.3352>.
- Brunden, K.R., Lee, V.M.-Y., Smith 3rd, A.B., Trojanowski, J.Q., Ballatore, C., 2017. Altered microtubule dynamics in neurodegenerative disease: Therapeutic potential of microtubule-stabilizing drugs. *Neurobiol. Dis.* 105, 328–335. <https://doi.org/10.1016/j.nbd.2016.12.021>.
- Dhar, G.A., Saha, S., Mitra, P., Nag Chaudhuri, R., 2021. DNA methylation and regulation of gene expression: guardian of our health. *Nucl. Biol.* 64, 259–270. <https://doi.org/10.1007/s13237-021-00367-y>.
- Di Tommaso, P., Chatzou, M., Floden, E.W., Barja, P.P., Palumbo, E., Notredame, C., 2017. Nextflow enables reproducible computational workflows. *Nat. Biotechnol.* <https://doi.org/10.1038/nbt.3820>.
- Dobin, A., Davis, C.A., Schlesinger, F., Drenkow, J., Zaleski, C., Jha, S., Batut, P., Chaisson, M., Gingeras, T.R., 2013. STAR: ultrafast universal RNA-seq aligner. *Bioinformatics* 29, 15–21. <https://doi.org/10.1093/bioinformatics/bts635>.
- Du, P., Zhang, X., Huang, C.C., Jafari, N., Kibbe, W.A., Hou, L., Lin, S.M., 2010. Comparison of Beta-value and M-value methods for quantifying methylation levels by microarray analysis. *BMC Bioinforma.* 11 <https://doi.org/10.1186/1471-2105-11-587>.
- Ehrlich, M., 2019. DNA hypermethylation in disease: mechanisms and clinical relevance. *Epigenetics* 14, 1141–1163. <https://doi.org/10.1080/15592294.2019.1638701>.
- Ewels, P.A., Peltzer, A., Fillinger, S., Patel, H., Alneberg, J., Wilm, A., Garcia, M.U., Di Tommaso, P., Nahnsen, S., 2020. The nf-core framework for community-curated bioinformatics pipelines. *Nat. Biotechnol.* <https://doi.org/10.1038/s41587-020-0439-x>.
- Hebestreit, K., Dugas, M., Klein, H.U., 2013. Detection of significantly differentially methylated regions in targeted bisulfite sequencing data. *Bioinformatics* 29, 1647–1653. <https://doi.org/10.1093/bioinformatics/btt263>.
- Hunt, R.F., Scheff, S.W., Smith, B.N., 2009. Posttraumatic epilepsy after controlled cortical impact injury in mice. *Exp. Neurol.* 215, 243–252. <https://doi.org/10.1016/j.expneurol.2008.10.005>.
- Jin, B., Li, Y., Robertson, K.D., 2011. DNA methylation: Superior or subordinate in the epigenetic hierarchy? *Genes Cancer* 2, 607–617. <https://doi.org/10.1177/1947601910393957>.
- Kandashvili, M., Gamkrelidze, G., Tsvetava, L., Lordkipanidze, T., Lepsveridze, E., Lagani, V., Burjanadze, M., Dashniani, M., Kokaia, M., Solomonias, R., 2022. Myo-inositol limits kainic acid-induced epileptogenesis in rats. *Int. J. Mol. Sci.* 23 <https://doi.org/10.3390/ijms23031198>.
- Kelly, K.M., Miller, E.R., Lepsveridze, E., Kharlamov, E.A., Mchedlishvili, Z., 2015. Posttraumatic seizures and epilepsy in adult rats after controlled cortical impact. *Epilepsy Res* 117, 104–116. <https://doi.org/10.1016/j.eplepsyres.2015.09.009>.
- Kenborg, L., Rugbjerg, K., Lee, P.C., Ravnskjær, L., Christensen, J., Ritz, B., Lassen, C.F., 2015. Head injury and risk for Parkinson disease: results from a Danish case-control study. *Neurology* 84, 1098–1103. <https://doi.org/10.1212/WNL.0000000000001362>.
- Kharlamov, E.A., Lepsveridze, E., Meparishvili, M., Solomonias, R.O., Lu, B., Miller, E.R., Kelly, K.M., Mchedlishvili, Z., 2011. Alterations of GABA(A) and glutamate receptor subunits and heat shock protein in rat hippocampus following traumatic brain injury and in posttraumatic epilepsy. *Epilepsy Res* 95, 20–34. <https://doi.org/10.1016/j.eplepsyres.2011.02.008>.
- Krueger, F., Andrews, S.R., 2011. Bismark: a flexible aligner and methylation caller for Bisulfite-Seq applications. *Bioinformatics* 27, 1571–1572. <https://doi.org/10.1093/bioinformatics/btr167>.
- Li, R., Shen, Y., 2013. An old method facing a new challenge: re-visiting housekeeping proteins as internal reference control for neuroscience research. *Life Sci.* 92, 747–751. <https://doi.org/10.1016/j.lfs.2013.02.014>.
- Love, M.I., Huber, W., Anders, S., 2014. Moderated estimation of fold change and dispersion for RNA-seq data with DESeq2. *Genome Biol.* 15, 1–21. <https://doi.org/10.1186/s13059-014-0550-8>.

- Masel, B.E., Scheibel, R.S., Kimbark, T., Kuna, S.T., 2001. Excessive daytime sleepiness in adults with brain injuries. *Arch. Phys. Med. Rehabil.* 82, 1526–1532. <https://doi.org/10.1053/apmr.2001.26093>.
- McLean, A.J., Dikmen, S., Temkin, N., Wyler, A.R., Gale, J.L., 1984. Psychosocial functioning at 1 month after head injury. *Neurosurgery* 14, 393–399. <https://doi.org/10.1227/00006123-198404000-00001>.
- Monsour, M., Gordon, J., Lockard, G., Alayli, A., Elsayed, B., Connolly, J., Borlongan, C. V., 2022. Minor changes for a major impact: a review of epigenetic modifications in cell-based therapies for stroke. *Int. J. Mol. Sci.* 23 <https://doi.org/10.3390/ijms232113106>.
- Mtchedlishvili, Z., Lepsveridze, E., Xu, H., Kharlamov, E.A., Lu, B., Kelly, K.M., 2010. Increase of GABAA receptor-mediated tonic inhibition in dentate granule cells after traumatic brain injury. *Neurobiol. Dis.* 38, 464–475. <https://doi.org/10.1016/j.nbd.2010.03.012>.
- Murphy, T.L., Tussiwand, R., Murphy, K.M., 2013. Specificity through cooperation: BATF-IRF interactions control immune-regulatory networks. *Nat. Rev. Immunol.* 13, 499–509. <https://doi.org/10.1038/nri3470>.
- Ngwenya, L.B., Danzer, S.C., 2019. Impact of traumatic brain injury on neurogenesis. *Front. Neurosci.* 13, 1–8. <https://doi.org/10.3389/fnins.2018.01014>.
- Olczak, M., Poniatowski, L., Kwiatkowska, M., Samojłowicz, D., Tarka, S., Wierzbabobrowicz, T., 2019. Immunolocalization of dynein, dynactin, and kinesin in the cerebral tissue as a possible supplemental diagnostic tool for traumatic brain injury in postmortem examination. *Folia Neuropathol.* 57, 51–62. <https://doi.org/10.5114/fn.2019.83831>.
- Osier, N.D., Dixon, C.E., 2016. The controlled cortical impact model: applications, considerations for researchers, and future directions. *Front. Neurol.* 7, 1–14. <https://doi.org/10.3389/fneur.2016.00134>.
- Patro, R., Duggal, G., Love, M.I., Irizarry, R.A., Kingsford, C., 2017. Salmon provides fast and bias-aware quantification of transcript expression. *Nat. Methods* 14, 417–419. <https://doi.org/10.1038/nmeth.4197>.
- Rakib, F., Al-Saad, K., Ahmed, T., Ullah, E., Barreto, G.E., Md Ashraf, G., Ali, M.H.M., 2021. Biomolecular alterations in acute traumatic brain injury (TBI) using Fourier transform infrared (FTIR) imaging spectroscopy. *Spectrochim. Acta - Part A Mol. Biomol. Spectrosc.* 248, 119189 <https://doi.org/10.1016/j.saa.2020.119189>.
- Ramesh, G., Maclean, A.G., Philipp, M.T., 2013. Cytokines and chemokines at the crossroads of neuroinflammation, neurodegeneration, and neuropathic pain. *Mediat. Inflamm.* 2013 <https://doi.org/10.1155/2013/480739>.
- Ratliff, W.A., Delic, V., Pick, C.G., Citron, B.A., 2020. Dendritic arbor complexity and spine density changes after repetitive mild traumatic brain injury and neuroprotective treatments. *Brain Res* 1746, 147019. <https://doi.org/10.1016/j.brainres.2020.147019>.
- Ritchie, M.E., Phipson, B., Wu, D., Hu, Y., Law, C.W., Shi, W., Smyth, G.K., 2015. limma powers differential expression analyses for RNA-sequencing and microarray studies. *Nucleic Acids Res* 43, e47. <https://doi.org/10.1093/nar/gkv007>.
- Smith, B.N., 2016. How and why study posttraumatic epileptogenesis in animal models? *Epilepsy Curr.* 16, 393–396. <https://doi.org/10.5698/1535-7511-16.6.393>.
- Solomonias, R., Gogichaishvili, N., Nozadze, M., Lepsveridze, E., Dzeladze, D., Kiguradze, T., 2013. Myo-inositol treatment and GABA-A receptor subunit changes after kainate-induced status epilepticus. *Cell. Mol. Neurobiol.* 33, 119–127. <https://doi.org/10.1007/s10571-012-9877-4>.
- Solomonias, R., Mikautadze, E., Nozadze, M., Kuchishvili, N., Lepsveridze, E., Kiguradze, T., 2010. Myo-inositol treatment prevents biochemical changes triggered by kainate-induced status epilepticus. *Neurosci. Lett.* 468, 277–281. <https://doi.org/10.1016/j.neulet.2009.11.012>.
- Taylor, M.J., Wilder, H., Bhagwagar, Z., Geddes, J., 2004. Inositol for depressive disorders. CD004049 *Cochrane Database Syst. Rev.* 2004. <https://doi.org/10.1002/14651858.CD004049.pub2>.
- Tsverava, L., Kandashvili, M., Margvelani, G., Lortkipanidze, T., Gamkrelidze, G., Lepsveridze, E., Kokaia, M., Solomonias, R., 2019. Long-term effects of myo-inositol on behavioural seizures and biochemical changes evoked by kainic acid induced epileptogenesis. *Biomed. Res. Int.* 2019, 4518160 <https://doi.org/10.1155/2019/4518160>.
- Tsverava, L., Lordkipanidze, T., Lepsveridze, E., Nozadze, M., Kikvidze, M., Solomonias, R., 2016. Myo-inositol attenuates the cell loss and biochemical changes induced by kainic acid status epilepticus. *Biomed. Res. Int.* 2016, 2794096 <https://doi.org/10.1155/2016/2794096>.
- Unfer, V., Facchinetti, F., Orrù, B., Giordani, B., Nestler, J., 2017. Myo-inositol effects in women with PCOS: a meta-analysis of randomized controlled trials. *Endocr. Connect.* 6, 647–658. <https://doi.org/10.1530/EC-17-0243>.
- Ustaoglu, S.G., Ali, M.H.M., Rakib, F., Bleser, E.L.A., Van Heijningen, C.L., Dijkhuizen, R. M., Severcan, F., 2021. Biomolecular changes and subsequent time-dependent recovery in hippocampal tissue after experimental mild traumatic brain injury. *Sci. Rep.* 11 (1), 13. <https://doi.org/10.1038/s41598-021-92015-3>.
- Vespa, P.M., 2013. Hormonal dysfunction in neurocritical patients. *Curr. Opin. Crit. Care* 19, 107–112. <https://doi.org/10.1097/MCC.0b013e32835e7420>.
- Wu, T., Hu, E., Xu, S., Chen, M., Guo, P., Dai, Z., Feng, T., Zhou, L., Tang, W., Zhan, L., Fu, X., Liu, S., Bo, X., Yu, G., 2021. clusterProfiler 4.0: a universal enrichment tool for interpreting omics data. *Innovation* 2, 100141. <https://doi.org/10.1016/j.xinn.2021.100141>.
- Yao, X., Liu, J., McCabe, J.T., 2008. Alterations of cerebral cortex and hippocampal proteasome subunit expression and function in a traumatic brain injury rat model. *J. Neurochem.* 104, 353–363. <https://doi.org/10.1111/j.1471-4159.2007.04970.x>.
- Zima, L., West, R., Smolen, P., Kobori, N., Hergenroeder, G., Choi, H.M.A., Moore, A.N., Redell, J.B., Dash, P.K., 2022. Epigenetic modifications and their potential contribution to traumatic brain injury pathobiology and outcome. *J. Neurotrauma*. <https://doi.org/10.1089/neu.2022.0128>.
- Zlotnik, A., Yoshie, O., 2000. Chemokines: a new classification system and their role in immunity. *Immunity* 12, 121–127. [https://doi.org/10.1016/s1074-7613\(00\)80165-x](https://doi.org/10.1016/s1074-7613(00)80165-x).
- Zsurka, G., Appel, M.L.T., Nastaly, M., Hallmann, K., Hansen, N., Nass, D., Baumgartner, T., Surges, R., Hartmann, G., Bartok, E., Kunz, W.S., 2023. Loss of the immunomodulatory transcription factor BATF2 in humans is associated with a neurological phenotype. *Cells* 12. <https://doi.org/10.3390/cells12020227>.